we have plotted the reduced temperatures and densities and also the critical ratios of various substances against λ and compared these with the results of our model.[9] In the case of the critical ratio there is experimentally an increase of about 5% as λ increases from Xe to He^3, whereas the model shows a decrease of 0.5% over the same range of λ. Thus our model agrees with the experiment by giving only a small variation of the critical ratio due to quantum effects. When the reduced critical temperatures and densities of the noble gases and hydrogen isotopes are plotted against λ, the agreement of the results with those of the model is remarkably good, especially for the dependence of critical density on λ.

[9] After completion of this paper M. E. Fisher supplied us with more recent experimental data collected by him for Ref. 4. However, use of those results makes only about 1% change to Fig. 2.

PHYSICAL REVIEW VOLUME 149, NUMBER 1 9 SEPTEMBER 1966

Temperature Dependence of the Structure of Liquid Indium*

H. OCKEN AND C. N. J. WAGNER
Hammond Laboratory, Yale University, New Haven, Connecticut
(Received 1 March 1966)

The x-ray diffraction pattern of liquid indium were measured at 170, 280, 390, 500, and 650°C. For comparison, liquid mercury was measured at room temperature. All data were taken with a θ-θ diffractometer from the open surface of the melt between values of $K=4\pi \sin\theta/\lambda=1.5$ and 15 Å^{-1}. Absolute intensity data $I_{e.u.}^{coh}$ were obtained by scaling the measured intensity of In to that of liquid mercury (coh=coherent, e.u. =electron units). The values of $I_{e.u.}^{coh}$ for $K>12$ did not show extensive modulation and were in good agreement with the square of the dispersion-corrected scattering factor f of In. The interference function $I(K)$ was calculated by dividing the $I_{e.u.}^{coh}$ values by the theoretical f^2 values. Fourier transform of $I(K)$ yielded the radial distribution function RDF$=4\pi r^2\rho(r)$ and pair probability function $g(r)=\rho(r)/\rho_0$, where ρ_0 is the atomic density. The RDF curve of Hg is completely free of ripples below $r<D$, where D is the hard-sphere diameter, indicating that $I_{e.u.}^{coh}$ and f^2 were determined accurately. In the case of In, ripples were found below the first peak in the RDF. We conclude that these ripples are a consequence of the use of inappropriate f^2 values rather than errors in $I_{e.u.}^{coh}$, since Hg and In were measured under identical conditions. Fourier transform of the ripple-free RDF yielded an $I(K)$ curve which was about 10% higher in the region of the first peak. Dividing $I_{e.u.}^{coh}$ by the corrected $I(K)$ leads to values of the scattering factor which are 5% lower in the range of $K=1.5$ to 8 Å^{-1} than the Dirac-Slater scattering factors. The distribution of the atoms in liquid In can be approximately described by the hard-sphere model with a packing density of 0.45 compared to 0.74 in the solid. This density corresponds to a hard-sphere diameter $D=2.86$ Å, which is the first value of r in the RDF where $\rho(r)=\rho_0$. The interatomic distances r_1 taken as the position of the first peak maximum in the RDF and the coordination number CN decrease with increasing temperature. Both variations are a consequence of the excess or free volume created in the liquid. The electrical resistivity ρ_R and thermoelectric power Q of liquid In were calculated from the measured I(K) and the theoretical values of the Fourier transform $U(K)$ of the pseudopotential for different temperatures. The predicted values of ρ_R are about 50% lower than those observed experimentally. The theory also underestimates the temperature dependence of the resistivity by about a factor of 3.

I. INTRODUCTION

THE liquid state of matter is the least understood of the three common states solid, liquid, and gaseous. The atomic arrangement in the liquid state represents a compromise between the long-range order characteristic of crystalline solids and total disorder characteristic of gases. There must be correlations between atoms separated by short distances in the liquid, but complete randomness between atoms or molecules separated by large distances.

The distribution of atoms as a function of the radial distance r about a given reference atom, i.e., $4\pi r^2\rho(r)$, can be obtained from the x-ray intensity $I_N(K)$ scattered by N atoms with scattering factors f as a function of the magnitude of the diffraction vector $K=4\pi(\sin\theta)/\lambda$, where 2θ is the angle between the incident and diffracted x rays and λ is the wavelength[1–3]:

$$4\pi r^2\rho(r)=4\pi r^2\rho_0+\left(\frac{2r}{\pi}\right)\int_0^\infty K[I(K)-1](\sin Kr)dK\,, \quad (1)$$

where ρ_0 is the average atomic density and $I(K)$ is the interference function given by

$$I(K)=I_N(K)/(Nf^2)=I_{e.u.}^{coh}(K)/f^2. \quad (2)$$

$I_{e.u.}^{coh}(K)$ is the coherent scattering from one atom in electron units.

* This paper is based on the D. Eng. thesis of H. Ocken submitted to the School of Engineering, Yale University, 1966.

[1] A. Guinier, *X-Ray Diffraction in Crystals, Imperfect Crystals, and Amorphous Bodies* (W. H. Freeman and Company, Inc., San Francisco, 1963).
[2] N. S. Gingrich, Rev. Mod. Phys. 15, 90 (1943).
[3] K. Furukawa, Rept. Progr. Phys. 25, 395 (1962).

The Fourier transform of Eq. (1) yields an expression for the interference function in terms of the radial distribution function (RDF):

$$I(K)=1+\int_0^\infty 4\pi r^2[\rho(r)-\rho_0]\frac{\sin Kr}{Kr}dr. \quad (3)$$

It is important to note that RDF and $I(K)$ are two different representations of the same information. The RDF provides a description in real or object space, while $I(K)$ represents a description of the atomic arrangment in reciprocal space. The passage from one space to the other is effected through Fourier transforms. In order to show this reciprocity more clearly and to facilitate the transformation operation, Kaplow, Strong, and Averbach[4] use the notation

$$F(K)=K[I(K)-1], \quad (4)$$

$$G(r)=4\pi r[\rho(r)-\rho_0]=4\pi r\rho_0[g(r)-1], \quad (5)$$

where $g(r)$ is the pair correlation function. Therefore, Eqs. (1) and (3) can be written as

$$G(r)=\left(\frac{2}{\pi}\right)\int_0^\infty F(K)(\sin Kr)dK, \quad (6)$$

$$F(K)=\int_0^\infty G(r)(\sin Kr)dr. \quad (7)$$

The RDF is of interest in the theories of the liquid state because, in conjunction with the knowledge of the intermolecular potential, the thermodynamic functions of the liquid can be specified. It also allows direct comparison with RDF's obtained from particular models of liquids, such as the hard-sphere model[5,6] or the long-range oscillatory-potential model.[7,8] The RDF's show fluctuation about the average atomic distribution $4\pi r^2\rho_0$. The maxima represent the preferred distances of separation between atoms in the liquid and the area under a peak gives the coordination number CN. These data can be directly compared with solid-state values, and provide some insight into the structural changes that occur upon melting.

In the last few years, the most exciting advances in the theory of metallic liquids have been related to a description of the transport properties.[9–11] Measurements of the Hall constants R of liquid metals have shown that they deviate very little from the value predicted by the free-electron theory,[12] i.e., $R=1/Ne$, where N is a number of conduction electrons per unit volume and e is the charge of the electron. The theoretical difficulties associated with the calculation of the transport parameters have been overcome by the introduction of the free-electron-like pseudo-wave function or pseudopotential, which describes the electron-ion interaction.

The electrical resistivity ρ_R can be calculated from the expression[9,10,13,14]

$$\rho_R=[3\pi(m^*)^2/(\hbar^3e^2k_F^2\rho_0)]\langle I(K)|U(K)|^2\rangle, \quad (8)$$

where m^* is the effective mass and e is the charge of the electron, $\hbar=h/2\pi$, h is the Planck constant, ρ_0 is the average atomic density, and k_F is the wave vector associated with the Fermi energy E_F, i.e.,

$$E_F=\hbar^2(3\pi^2N)^{2/3}/(2m^*)=\hbar^2k_F^2/(2m^*). \quad (9)$$

$N=\zeta\rho_0$ is the number of valence electrons per unit volume and ζ is the number of valence electrons per atom. The average value of $\langle I(K)|U(K)|^2\rangle$ is defined as

$$\langle I(K)|U(K)|^2\rangle=4\int_0^1 I(K)|U(K)|^2\times\left(\frac{K}{2k_F}\right)^3 d\left(\frac{K}{2k_F}\right). \quad (10)$$

As shown by Ziman,[13] this approach also yields a theoretical expression for the thermoelectric power Q;

$$Q=[-\pi^2k^2T/(3|e|E_F)][3-2I(2k_F)\times|U(2k_F)|^2/\langle I(K)|U(K)|^2\rangle], \quad (11)$$

where k is the Boltzmann constant and T is the absolute temperature.

In principal, we should be able to calculate the electrical resistivity and thermoelectric power of liquid metals directly from the above equations. In practice, one is often hampered by the lack of accurate values of the interference function $I(K)$ and the transform of the pseudopotential $U(K)$.

Any experimental study of the liquid state is likely to be hindered to varying degrees by high vapor pressures, chemical reactivity of the sample with the container, and high temperatures. X-ray-diffraction studies, which provide a direct means for determining the atomic arrangement in liquids, are particularly hampered by the weak intensities characteristic of the scattering from liquids. Early investigations, which were generally motivated by a desire to obtain a knowledge of interatomic distances and coordination numbers, often show significant variations in the interference functions at small values of K. As such discrepancies have little effect on the RDF, the quantities of interest could be

[4] R. Kaplow, S. L. Strong, and B. L. Averbach, Phys. Rev. **138**, A1336 (1965).
[5] N. W. Ashcroft and J. Lekner, Phys. Rev. **145**, 83 (1966).
[6] M. S. Wertheim, Phys. Rev. Letters **10**, 321 (1963).
[7] A. Paskin and A. Rahman, Phys. Rev. Letters **16**, 300 (1966).
[8] J. E. Enderby and N. H. March, Advan. Phys. **14**, 453 (1965).
[9] J. M. Ziman, Phil. Mag. **6**, 1013 (1961).
[10] C. C. Bradley, T. E. Faber, E. G. Wilson, and J. M. Ziman, Phil. Mag. **7**, 865 (1962).
[11] N. E. Cusack, Rept. Progr. Phys. **26**, 361 (1963).
[12] J. E. Enderby, Proc. Phys. Soc. (London) **81**, 772 (1963).
[13] L. J. Sundström, Phil. Mag. **11**, 657 (1965).
[14] N. W. Ashcroft and L. J. Guild-Sundström, Phys. Letters **14**, 23 (1965).

obtained quite accurately. On the other hand, the transport properties are extremely sensitive to the details of the interference function at low values of K. Only recently has some measure of reproducibility been achieved in the measurement of the low-angle region of the interference function. Pfannenschmid,[15] Kaplow *et al.*,[4] Wagner *et al.*,[16] and Black and Cundall[17] report interference functions of liquid mercury which agree to $\pm 7\%$ in the region of the first maxima. We therefore propose that measurements of the scattering from this element be used as the basis for the comparison of the diffraction patterns of liquids obtained at different laboratories.

In view of the difficulties surrounding the x-ray diffraction studies of liquids, it is not surprising that there have been few investigations of the temperature dependence of the structure of liquids. Including neutron-diffraction measurements, the only metallic elements which have been investigated over a large temperature range are mercury,[18] rubidium,[19] cesium,[19] and tin.[20]

In this paper we present a study of the temperature dependence of the x-ray scattering from liquid indium. An extensive comparison of theoretical and experimental values of the electrical resistivity and thermoelectric power of liquid metals by Sundström[13] presented no such calculation for indium. Using interference functions based on a hard-sphere model of a liquid, Ashcroft and Lekner[5] compare theoretical and experimental resistivities just above the melting point. Measurements over a range of temperatures will provide a means for obtaining a theoretical value of the temperature coefficient of the resistivity. Such a quantity will provide a more severe test of the pseudopotential approach than has hitherto been available. To insure a high degree of accuracy, measurements will be made using a focusing θ-θ diffractometer and a scintillation detector. Particular attention will be paid to factors affecting the measured intensities and their conversion to absolute units. Measurements will be standardized against the scattering from liquid mercury at room temperature. The data should also enable the somewhat surprising discrepancies which have been reported in the RDF of liquid indium to be resolved. Gamertsfelder,[21] Kim *et al.*,[22] and Orton[23] give a value of the first preferred separation distance $r_1=3.30$ Å, whereas Hendus[24] and Knosp[25] obtain $r_1=3.17$ and 3.15 Å, respectively.

II. EXPERIMENTAL PROCEDURE

The experimental arrangement for the measurement of the scattered x-ray intensities from the liquid was identical to the one described by Wagner *et al.*[16] The focusing diffraction geometry was realized with a θ-θ diffractometer which allows the measurement of the scattered x rays from the open surface of the liquid. A quartz-crystal monochromator in the diffracted beam was used to eliminate the white spectrum, the K_β radiation, most of the Compton scattering, and the fluorescent radiation from the sample.

Indium of 99.99% purity was heated in a graphite crucible (25×20 mm^2) and He–20% H mixture in the high-temperature camera.[26] Before each run the indium sample was heated to 800°C, where any oxide was quickly reduced by the protective atmosphere, and then brought to the temperature of the measurements. Alignment of the sample into the diffractometer axis and calibration of the high temperature camera have been described previously.[16] Measurements were made at 170, 280, 390, 500, and 650°C±5°C.

All data were obtained with Mo radiation using a 0.54° divergence slit, a 0.14° receiving slit and no Soller slits. Scatter shields above the sample and the monochromator crystal and scatter slits in the diffracted beam served to minimize extraneous scattering. The time required to count 4000 x-ray pulses was registered at intervals of 0.2° between 8° and 20°, 0.5° between 20° and 80°, and 1° between 80° and 125° in 2θ. This angular range corresponds to $K_{\min}=1.5$ Å^{-1} to $K_{\max}=15.7$ Å^{-1}. The reported data below 20° in 2θ correspond to an average of three runs at each temperature.

III. ANALYSIS AND RESULTS

The interference and radial distribution functions were determined from the measured intensities with the aid of a FORTRAN program compiled for use with an IBM 7040-7094 computer. After subtracting the counter noise, the measured intensities I_{meas} were divided by the proper polarization and absorption factors,

$$PA=[(1+\cos^2 2\alpha\cos^2 2\theta)/(1+\cos^2 2\alpha)]/2\mu,$$

where 2α is the diffraction angle of the monochromator and μ is the linear absorption coefficient (see Table I[27]). The corrected intensities $I_{\text{cor}}=I_{\text{meas}}/PA$ are proportional to the sum of the coherently scattered radiation

[15] O. Pfannenschmid, Z. Naturforsch. **15a**, 603 (1960).
[16] C. N. J. Wagner, H. Ocken, and M. L. Joshi, Z. Naturforsch. **20a**, 325 (1965).
[17] P. J. Black and J. A. Cundall, Acta Cryst. **19**, 807 (1965).
[18] J. A. Campbell and J. H. Hildebrand, J. Chem. Phys. **11**, 330 (1943).
[19] N. S. Gingrich and L. Heaton, J. Chem. Phys. **34**, 873 (1961).
[20] K. Furukawa, B. R. Orton, J. Hamor, and G. I. Williams, Phil. Mag. **8**, 141 (1963).
[21] C. Gamertsfelder, J. Chem. Phys. **9**, 450 (1941).
[22] Y. S. Kim, C. L. Standley, R. F. Kruh, and G. T. Clayton, J. Chem. Phys. **34**, 1464 (1961).
[23] B. R. Orton, Ph.D. thesis, University of London, 1964 (unpublished).
[24] H. Hendus, Z. Naturforsch. **2a**, 505 (1947).
[25] H. Knosp, Dipl. Arbeit, Techn. Hochschule, Stuttgart, 1964 (unpublished).
[26] M. L. Joshi, Rev. Sci. Instr. **36**, 678 (1965).
[27] P. J. McGonigal, J. A. Cahill, and A. D. Kirshenbaum, J. Inorg. Nucl. Chem. **24**, 1012 (1962).

TABLE I. The mass absorption coefficients (μ/ρ) for Mo $K\alpha$ radiation, the mass densities ρ,[a] and the atomic densities ρ_0 of Hg and In at different temperatures.

Element	Temp (°C)	μ/ρ (cm²/g)	ρ (g/cm³)	ρ_0 (Å⁻³)
Hg	28	132	13.55	0.0407
In	170	31.8	7.014	0.0368
	280	31.8	6.939	0.0364
	390	31.8	6.864	0.0360
	500	31.8	6.790	0.0356
	650	31.8	6.688	0.0351

[a] Reference 27.

$I_{\text{e.u.}}^{\text{coh}}$ and Compton radiation $I_{\text{e.u.}}^{\text{inc}}$ in electron units, i.e.,

$$I_{\text{cor}}=I_{\text{meas}}/(PA)=\Phi\rho_0(I_{\text{e.u.}}^{\text{coh}}+I_{\text{e.u.}}^{\text{inc}}), \quad (12)$$

$$I_{\text{e.u.}}^{\text{coh}}=\beta I_{\text{cor}}-I_{\text{e.u.}}^{\text{inc}}, \quad (13)$$

where $\beta=1/(\Phi\rho_0)$ is the normalization constant. The product of $\beta\rho_0=1/\Phi$ is independent of the liquid sample and depends only on the experimental arrangement.[16] Values of the average atomic density ρ_0 were calculated from the macroscopic densities[28] and are shown in Table I. The values of β, shown in Table II, were obtained with the high-angle method (β_h) and the modified radial-distribution-function method (β_{RDF}), hitherto referred to as the modified Krogh-Moe and Norman method.[3,16] The atomic scattering factors used in the analysis were those of Cromer and Waber[28] and the dispersion corrections were those of Cromer.[29] The two normalization constants were identical in the case of Hg, but β_h was always smaller than β_{RDF} in the case of In. The difference was still less than 2%. Using the value of β(Hg), we obtained a value of β(In):

$$\beta(\text{In})=\beta(\text{Hg})\rho_0(\text{Hg})/\rho_0(\text{In}). \quad (14)$$

This value was about 1% smaller than β_h(In), indicating that the measured intensities and the theoretical scattering factors were quite accurate for larger values of K, i.e., $K>10$ Å^{-1}. The difference between β_h and β_{RDF} for In must be due to the particular choice of the dispersion corrected scattering factors at smaller values of K.

Values given by Sagel[30] were used to account for the Compton incoherent scattering. Positioning the quartz crystal monochromator in the diffracted beam results in the Compton radiation being eliminated when the resolving power of the monochromator is greater than the wavelength shift of the Compton radiation. An estimate of this cutoff point was obtained by measuring the dispersion profile as a function of wavelength after reflection of the primary beam from a single crystal of NaCl in the sample position. The wavelength spread

TABLE II. Representative values of the square of the dispersion-corrected atomic-scattering factors. (C&W) denote values obtained using the uncorrected atomic-scattering factors of Cromer and Waber (Ref. 28). The last column gives values for indium deduced from the refinement procedure. The dispersion corrections used were those of Cromer (Ref. 29).

K	Hg(C&W)	In(C&W)	In
0	6055	2318	2318
2	4852	1727	1610
4	3286	1066	1003
6	2245	661	625
8	1596	445	431
10	1166	328	325
12	865	254	256
14	650	196	199

was then related to the resolving power of the crystal using the penetration aberration analysis of Scott.[31] For the quartz crystal in question the cutoff point was found to occur at $2\theta=18°$ or K$=2.8$ Å^{-1}.

The interference function $I(K)$ was obtained by dividing the coherently scattered intensity $I_{\text{e.u.}}^{\text{coh}}$ per atom in electron units by the square of the dispersion-corrected scattering factors. At small values of K, i.e., $K<1.5$ Å^{-1}, where measurements were unobtainable, $I(K)$ was smoothly extrapolated to $K=0$ using the relation[1]

$$I(0)=kT\rho_0K_\beta, \quad (15)$$

where k is the Boltzmann constant, T is the absolute temperature, and K_β is the isothermal compressibility. Values of K_β given by Hill[32] were used to calculate the value of $I(0)$.

The function $F(K)=K[I(K)-1]$ can then be generated from the interference function $I(K)$. Usually the values of $F(K)$ at large values of K are the least reliable because any error in $I(K)$ is magnified by the factor K. One must remember that $I(K)$ at large values of K is the quotient of two small quantities $I_{\text{e.u.}}^{\text{coh}}$ and f^2 which may not be too reliably known. To prevent the high angle or large K value region of $F(K)$ from assuming a disproportionate influence in the Fourier transform, $F(K)$ was weighted by a factor $\exp[-\sigma K^2]$, where σ was chosen to be zero and 0.005. When the differences between $I_{\text{e.u.}}^{\text{coh}}(K)$ and f^2 were on the order of the error resulting from counting statistics, $F(K)$ was arbitrarily set equal to zero. This value of $K_{\max}$ was always larger than 12.0 Å^{-1}.

The interference functions of In for different temperatures are shown in Fig. 1 and are tabulated in Table III for $1.0<K<3.0$ Å^{-1}. The corresponding radial distribution functions are represented in Fig. 2. For comparison, the $I(K)$ and $4\pi r^2\rho(r)$ of Hg measured at room temperature are shown in Fig. 3. The RDF are those obtained from $I(K)$ terminated at $K_{\max}=12.5$ Å^{-1} and no damping factor applied. Values of the inter-

[28] D. T. Cromer and J. T. Waber, Acta Cryst. **18**, 104 (1965).
[29] D. T. Cromer, Acta Cryst. **18**, 17 (1965).
[30] K. Sagel, *Tabellen zur Röntgenstrukturanalyse* (Springer-Verlag, Berlin, 1958).
[31] R. E. Scott, Rev. Sci. Instr. **35**, 118 (1964).
[32] J. E. Hill, M.S. thesis, Cornell University, 1965 (unpublished).

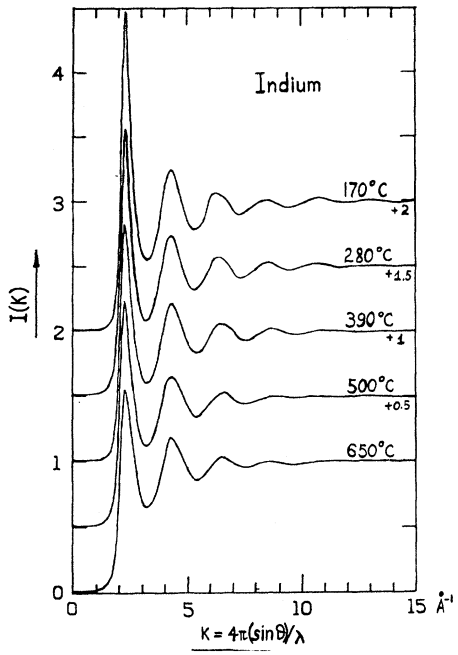

FIG. 1. Interference functions $I(K)$ of liquid indium for different temperatures. The values of $I(K)$ were obtained by dividing the absolute intensities $I_{e.u.}^{coh}(K)$ per atom by the square of dispersion corrected scattering factors of Cromer and Waber (Refs. 28,29).

TABLE III. Interference functions $I(K)$ of liquid mercury and liquid indium, calculated from the measured x-ray intensities and the dispersion corrected scattering factors of Cromer and Waber (Ref. 28).

	Hg	Indium				
Temp. °C	28	170	280	390	500	650
K	$I(K)$	$I(K)$	$I(K)$	$I(K)$	$I(K)$	$I(K)$
0	0.006	0.006	0.008	0.010	0.012	0.016
1.0	0.021	0.007	0.009	0.012	0.014	0.016
1.1	0.026	0.009	0.011	0.013	0.015	0.018
1.2	0.033	0.012	0.013	0.016	0.018	0.021
1.3	0.040	0.017	0.019	0.022	0.024	0.027
1.4	0.049	0.024	0.026	0.031	0.034	0.040
1.5	0.060	0.035	0.040	0.046	0.052	0.061
1.6	0.076	0.053	0.060	0.071	0.078	0.093
1.7	0.107	0.084	0.093	0.109	0.128	0.140
1.8	0.188	0.133	0.154	0.180	0.211	0.218
1.9	0.301	0.257	0.281	0.306	0.337	0.373
2.0	0.542	0.504	0.524	0.566	0.635	0.677
2.1	1.095	1.045	1.031	1.030	1.060	1.023
2.2	1.898	2.048	1.636	1.586	1.512	1.371
2.3	2.476	2.486	2.056	1.841	1.747	1.565
2.4	2.219	2.127	1.794	1.716	1.638	1.481
2.5	1.871	1.607	1.441	1.451	1.395	1.323
2.6	1.606	1.271	1.182	1.227	1.205	1.166
2.7	1.372	1.019	1.027	1.028	1.050	1.047
2.8	1.158	0.857	0.879	0.890	0.916	0.915
2.9	0.965	0.734	0.746	0.764	0.792	0.798
3.0	0.766	0.637	0.650	0.689	0.698	0.705

atomic distance r_1, obtained from both the RDF and the pair distribution function $g(r)$ and the coordination number CN, are given in Table IV. The interatomic distances were obtained by extrapolating the midpoints of the peak to the peak maximum. The values obtained in this manner from the RDF are about 0.05 Å larger than the values obtained from $g(r)$. The area under the RDF from $r=0$ to $r=r_{min}$, which is the position of the minimum value of the RDF after the first peak, was taken as the coordination number.

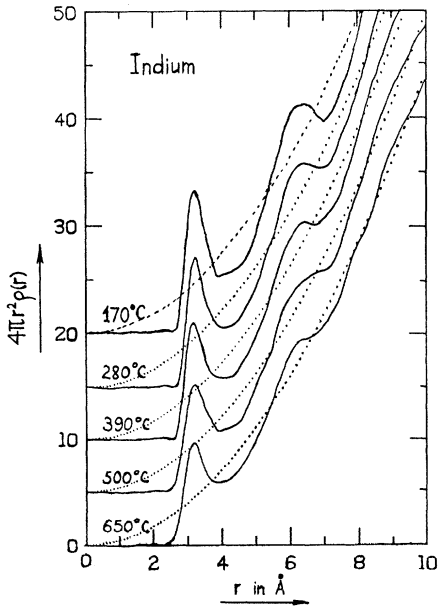

FIG. 2. Radial distribution functions $4\pi r^2\rho(r)$ of liquid indium for different temperatures obtained from the refined interference functions.

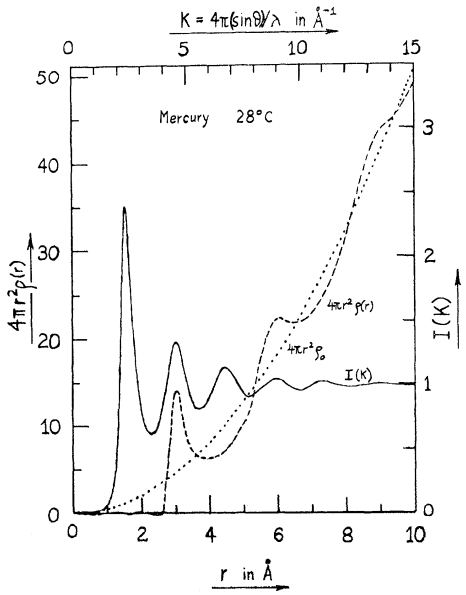

FIG. 3. Interference function $I(K)$ and radial distribution function of mercury at 28°C.

TABLE IV. The first preferred distance of separation r_1 determined from the functions $g(r)=\rho(r)/\rho_0$ and $4\pi r^2\rho(r)$ using different values of the upper limit of integration K_{max} and of the modification function $M(K)=\exp(-\sigma K^2)$. CN is the nearest-neighbor coordination number.

	K_{max}		$g(r)$			$4\pi r^2\rho(r)$		CN$_{meas.}$	CN$_{calc.}$
	σ	12.5	12.5	7.5	12.5	12.5	7.5		
		0	−0.005	0	0	−0.005	0		
Element	Temp (°C)		r_1'(Å)			r_1(Å)		(atoms)	
Hg	28	3.02	3.03	3.07	3.06	3.07	3.12	10.0	10.1
In	170	3.16	3.17	3.22	3.20	3.23	3.27	10.5	10.2
	280	3.13	3.14	3.19	3.18	3.20	3.25	10.1	9.8
	390	3.11	3.13	3.17	3.16	3.18	3.23	9.9	9.7
	500	3.12	3.13	3.17	3.18	3.19	3.24	9.7	9.6
	650	3.12	3.13	3.16	3.18	3.19	3.24	9.4	9.5

Using values of $U(K)$ given by Animalu,[33] the electrical resistivity and thermoelectric power were calculated for liquid In as a function of temperature and are given in Table V.

IV. DISCUSSION

A. Error Analysis

The radial distribution functions usually show erroneous features. The primary source of such errors are incorrect measurements of the x-ray intensity scattered by the liquid, use of incorrect values for the normalization constants and the atomic-scattering factor, and termination of the Fourier transform at a finite value of $K=K_{max}$ due to limitations imposed by the wavelength of the chosen x rays.

The termination of series error has been discussed extensively in the literature. It produces spurious ripples on both sides of the peaks of the RDF at a distance $\Delta r\approx\pm 8/K_{max}$ from the peak maximum position.[3] By varying the value of K_{max} one is able to distinguish these spurious peaks from those caused by other errors.

In order to reduce the spurious peaks in the RDF, $F(K)$ can be weighted by a modification function $M(K)=\exp(-\sigma K^2)$. In this way, errors in $F(K)$ at larger values of K do not have too large an influence in the Fourier transform. However, small shifts to larger distances r in the position of the first peak maximum of the RDF (i.e., the interatomic distance r_1) result from the use of this modification function. This is similar to the effect of decreasing the values of K_{max} in the Fourier integral which also produces shifts in r_1 to larger values of r as shown in Table IV. The change in interatomic distance r_1 is smaller when a mild modification function $M(K)=\exp(-0.005\ K^2)$ is applied to $F(K)$ terminated at $K_{max}=12.5$ Å^{-1} as compared to the shift resulting from the termination at $K_{max}=7.5$ Å^{-1} and the application of $M(K)=1$. This observation makes possible an interpretation of the discrepancies reported for the first preferred distance of separation of liquid indium in the recent investigations. A larger value of $r_1=3.30$ Å is expected in Orton's work,[23] where the use of Cu$K\alpha$ radiation limits K_{max} to approximately 7.5 Å^{-1}. Although Mo$K\alpha$ was used in the study by Kim *et al.*,[22] their application of a strong modification function $M(K)$, indicated by the extremely broad peaks in the RDF, will again result in a shift of r_1 to larger value $r_1=3.30$ Å. The value of $r_1=3.18$ Å at 280°C, obtained in the present investigation, is in excellent agreement with those obtained by Hendus[24] and Knosp.[25]

Any spurious ripples in the RDF which are clearly detectable at $r<D$ can be removed following the procedure outlined by Kaplow *et al.*[4] As the Fourier transform of the experimentally determined interference function of liquid mercury yielded a RDF which was almost completely free of ripples at small values of r, the refinement procedure was not applied to these data. The absence of noise at $r<D$ indicates that both the measured intensities and the theoretical atomic-scattering factors were determined to a high degree of accuracy. This conclusion is supported by applying Rahman's reliability criterion[34] to the measured x-ray intensities of Hg. Good agreement was found between the theoretical and experimental values.

The Fourier transformation of the indium data, however, yielded RDF's characterized by ripples at $r<D$.

TABLE V. The electrical resistivity and thermoelectric power of liquid indium. ρ_{obs} refers to the experimental values of Roll and Motz (Ref. 48). ρth(1) and Qth are the predicted values obtained using the experimentally determined interference functions. ρth(2) are the predicted values using the refined interference functions. Q_{obs} are the experimental values of Bradley (Ref. 50), taken from his figure.

Temp. (°C)	Resistivity ($\mu\Omega$ cm) ρ_{obs}	ρth(1)	ρth(2)	Thermoelectric power (μV/°K) Q_{obs}	Qth
170	33.5	22.6	24.3	···	0.59
280	36.3	22.3	23.9	···	0.90
390	39.1	23.1	24.7	−1.0	1.12
500	41.9	24.0	25.7	−1.2	1.11
650	45.7	24.3	26.0	−2.0	1.14

[33] A. O. E. Animalu, Cambridge University, Cavendish Laboratory Technical Report No. 3 1965 (unpublished).

[34] A. Rahman, J. Chem. Phys. 42, 3540 (1965).

The shape of these ripples was the same at all temperatures, indicating that they arose from a systematic error. Applying the refinement procedure to the indium data obtained at 170°C indicated that the interference function in the region of the first maximum should be about 10% higher than that obtained from the direct analysis of the data. The source of the discrepancy can be readily identified if we realize that in addition to RDF being equal to zero for $r<D$, a refined $I(K)$ for indium must result for which $\beta(\text{In})\rho_0(\text{In})=\beta(\text{Hg})\rho_0(\text{Hg})$, and the normalization constants determined by the two methods must be equal, i.e., $\beta_h=\beta_{\text{RDF}}$. These three conditions are mutually satisfied only if the differences between the initial and refined interference functions are ascribed to the use of theoretical values of the atomic-scattering factor of indium which are too high at small values of K. In accordance with this conclusion, the difference between β_h and β_{RDF} could be resolved. The belief that the discrepancy is not due to a systematic error in the measurement of the scattered intensities is based in part on our ability to accurately measure the scattering from liquid mercury under identical experimental conditions.

B. Atomic Scattering Factor of Indium

The calibration of the primary beam intensity from the measurements of the x-ray scattering of liquid mercury provides an alternate method for normalizing the indium data. As shown above, the product $\beta\rho_0=1/\Phi$ is independent of the sample [Eq. (14)]. Using this value of the normalization constant, we obtain the scattering intensity $I_{\text{e.u.}}^{\text{coh}}$ per atom in electron units. At values of $(\sin\theta)/\lambda>0.8$ Å^{-1} the modulations in $I_{\text{e.u.}}^{\text{coh}}$ have died out, and $I_{\text{e.u}}^{\text{coh}}$ should be equal to the dispersion-corrected f^2 values. The experimental values of the atomic scattering factor of indium obtained by dividing $I_{\text{e.u.}}^{\text{coh}}$ by $I(K)$ which yielded a ripple-free RDF are compared with theoretical atomic-scattering factors calculated from different atomic models in Fig. 4. Cromer[35] has shown that the Dirac-Slater (DS) model of the atom leads to the most compact charge density near the nucleus, thus resulting in the highest values of f at larger values of $(\sin\theta)/\lambda$. The DS atom represents the most sophisticated approach to the problem of the calculation of atomic-charge densities. The experimental values of the high-angle-scattering factor of indium, determined from the x-ray scattering of the liquid, agree with these theoretical calculations to within 1%.

This approach does assume, however, that the atomic scattering factor of mercury is accurately known, especially at values of $(\sin\theta)/\lambda>0.8$ Å^{-1}. Liberman *et al.*[36] have shown that the eigenvalues computed for Dirac-Slater (DS) wave functions are in better agreement with experimental x-ray energy levels than are any other scattering factors. For the case of mercury, agreement between experimental and theoretical energy levels for the inner shells, which are most significant in determining the atomic-scattering factor at high angles, is better than ½%. The absence of ripples in the RDF of mercury at $r<D$ provides other experimental evidence of the accuracy of the DS model. Similar results have been obtained for liquid Tl.[37]

The error analysis, presented above, indicated that the theoretical scattering factors below $(\sin\theta)/\lambda=0.8$ Å^{-1} were too high. The ratio of the intensity $I_{\text{e.u.}}^{\text{coh}}$ per atom and the refined interference function $I(K)$, which

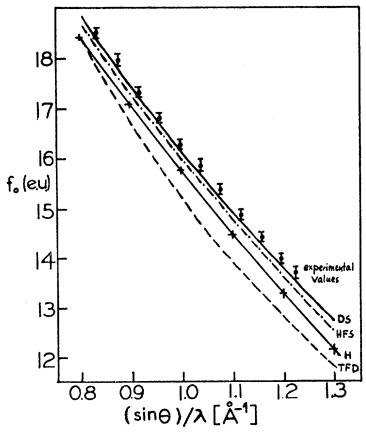

FIG. 4. High-angle atomic scattering factor of indium. The dots with error bars represent the experimental values using the scattering from liquid mercury as a standard. The theoretical scattering factors using the Thomas-Fermi-Dirac (TFD), Hartree (H), Hartree-Fock-Slater (HFS), and Dirac-Slater (DS) models are also given.

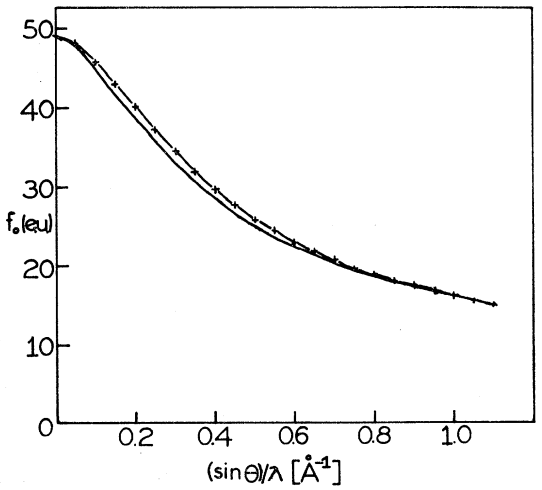

FIG. 5. Atomic scattering factors of indium. Curve (—+—+—) corresponds to the values of Cromer and Waber (Ref. 28); curve (———) corresponds to the values deduced from x-ray scattering from liquid indium.

[35] D. T. Cromer, Acta Cryst. **18**, 224 (1965).
[36] D. Liberman, J. T. Waber, and D. T. Cromer, Phys. Rev. **137**, A27 (1965).
[37] N. C. Halder and C. N. J. Wagner, J. Chem. Phys. **45**, 482 (1966).

yielded ripple-free RDF, is equal to the square of the dispersion-corrected scattering factor f_{expt}. The values of f_{expt} are shown in Fig. 5 together with the Dirac-Slater values of f_0 of Cromer and Waber.[28] The deviation between f_{expt} and f_0 is about 5%. Similar deviations between theoretically and experimentally determined scattering factors have been observed in solid copper, aluminum, and iron by Batterman *et al.*,[38] and in solid chromium by Cooper.[39] On the other hand, experimental studies of f_0 in rare gases by Chipman and Jennings[40] give results which are in excellent agreement with theoretical Hartree-Fock calculations. We therefore conclude that the discrepancies noted in liquid and solid metals are due to bonding effects.

C. Structure of Liquid Indium

The interatomic distance obtained from the RDF can be used with the density data to calculate the packing density of liquid indium just above the melting point. The packing density represents the ratio of the total volume occupied by the liquid to the volume occupied by the atoms. The former quantity is given by $v_0=1/\rho_0$ and the latter by $v_1=\pi r_1^3/6$, where r_1 is the atomic diameter obtained from the RDF. The ratio v_0/v_1 for liquid indium at 170°C is 1.65, which is identical to the value calculated by Furukawa[41] for a quasi-face-centered-cubic lattice model of a liquid. The random packing of spherical balls has been studied by Scott,[42] who obtained packing densities in the range from 1.59 to 1.70. That indium exhibits "closest-packing" in the liquid state can be taken as evidence that the partial covalent bonding present in the solid state is destroyed upon melting. Measurements of the transport properties of indium in the liquid state also support this view. The interatomic distance of indium can therefore be obtained from the preferred distance of separation in the liquid state after extrapolation to twelve-fold coordination. Such a procedure seems more reasonable than the indirect approaches used to obtain the interatomic distances of this element from solid-state measurements. The value so obtained from the liquid-state measurements is 3.20 Å, which compares well with the values of 3.32, 3.14, and 3.1 Å, given by Pauling,[43] Goldschmidt,[44] and Slater,[45] respectively.

With the assumption that liquid indium consists of a relatively close packing of atoms of density ρ_0, we can calculate the coordination number CN from values of the interatomic distance r_1. As shown by Furukawa,[41] the coordination number CN is given by

$$\text{CN(calc)}=6\sqrt{2}\rho_0 r_1^3. \tag{16}$$

Values of CN(calc) using the above equation are shown in Table IV. The agreement between the measured and calculated values is remarkably good.

A comparison of the measured interference function $I(K)$ for In at 170°C with that obtained from the hard-sphere model[5] using a packing parameter $\eta=\pi\rho_0 D^3/6=0.45$ shows that the two curves coincide reasonably well with each other for $K<2k_F$. The value of $\eta=0.45$ corresponds to $D=2.86$ Å. The closest packing of spheres would yield a value of $\eta_c=0.74$. Therefore, the ratio of η_c/η is equal to 1.65 and identical to the value calculated by Furukawa[41] for a quasi-face-centered-cubic lattice model of the liquid. The hard-sphere diameter $D=2.86$ Å is very close to the first distance r of the ripple-free RDF where $\rho(r)=\rho_0$. Calculations by Paskin and Rahman[7] indicate that the hard-sphere model does not yield a theoretical RDF for liquid Na near the melting point which would agree with the experimentally observed RDF. Application of long-range oscillatory potentials, however, improved the agreement considerably.

The somewhat surprising result that the preferred distance of separation decreases with increasing temperature can be readily explained. Following the approach used by Simmons and Balluffi[46] to calculate the vacancy concentration in solids, we can calculate the change in interatomic distance by subtracting from the macroscopic thermal expansion α_m the effects due to the generation of free volume α_f:

$$\Delta r_1=(r_1/3)(\Delta V_m/V_m-\Delta V_f/V_f)=r_1(\alpha_m-\alpha_f)\Delta T. \tag{17}$$

The first term can be calculated from the temperature dependence of the density and the second from the decrease of the coordination number with temperature:

$$\alpha_f=(-1/3)(1/CN)(\Delta CN/\Delta T). \tag{18}$$

The two expansivities α_m and α_f are shown in Fig. 6 together with their sum; the crosses mark the values of the preferred distances of separation determined directly from the RDF's. Both experimental and predicted results indicate a decreasing first-preferred distance of separation with temperature. The observations can be summarized by stating that the contraction of the atoms in the liquid due to the decrease in coordination number plays a more important role than the thermal expansion in determining the interatomic distance. A decreasing interatomic distance with increasing temperature is also predicted for the hard-sphere model of a liquid.

---

[38] B. W. Batterman, D. R. Chipman, and J. J. DeMarco, Phys. Rev. **122**, 68 (1961).
[39] M. J. Cooper, Phil. Mag. **7**, 2059 (1962).
[40] D. R. Chipman and L. D. Jennings, Phys. Rev. **132**, 728 (1963).
[41] K. Furukawa, Sci. Rep. Res. Inst. Tohoku Univ. Ser. A **12**, 368 (1960).
[42] G. D. Scott, Nature **188**, 908 (1960).
[43] L. Pauling, Proc. Roy. Soc. (London) **A114**, 181 (1927).
[44] V. M. Goldschmidt, Trans. Faraday Soc. **25**, 253 (1929).
[45] J. C. Slater, *Quantum Theory of Molecules and Solids* (McGraw-Hill Book Company, Inc., New York, N. Y., 1965), Vol. 2.
[46] R. D. Simmons and R. W. Balluffi, Phys. Rev. **125**, 862 (1962).

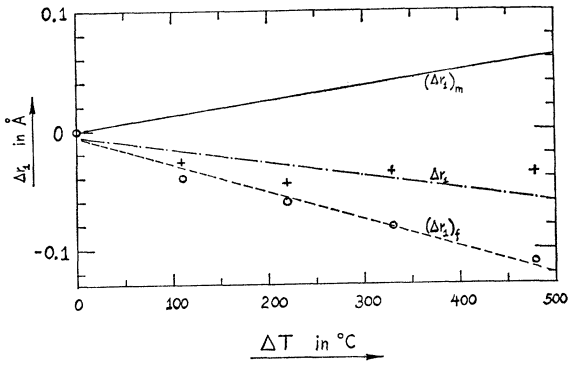

FIG. 6. The change Δr_1 in interatomic distance r_1 with temperature. $(\Delta r_1)_m=\alpha_m\Delta T$ is the change calculated from the macroscopic expansivity. $(\Delta r_1)_f=\alpha_f\Delta T$ is the change due to the generation of free volume. Δr_1 is the sum of the two preceding terms, i.e., $\Delta r_1=(\alpha_m-\alpha_f)\Delta T=(\Delta r_1)_m+(\Delta r_1)_f$. The crosses represent the experimental change Δr_1 obtained from position of the first peak maximum in the RDF.

D. Electron Transport Properties of Liquid Metals

The pseudopotential approach provides a means for computing the electronic-transport properties of liquid metals. Rather than solving the Schrödinger equation with the true ion potential, the orthogonality condition that the solution of the conduction states of an electron must be orthogonal to the core states can be made to look like a potential. This net effective ion-electron potential or pseudopotential is quite small, enabling it to be treated by standard perturbation theory.

Using Animalu's values[33,47] of the Fourier transforms of the pseudopotential $U(K)$, the resistivity and thermoelectric power calculated from the pseudopotential formulation are significantly different from the experimentally determined values. Just above the melting point the resistivity is about 50% lower than that observed by Roll and Motz[48] and Scala and Robertson.[49] The theory also considerably underestimates the temperature coefficient of the resistivity. The predicted value is $0.75\pm0.10\times10^{-2}$ $\mu\Omega$ cm/°K, whereas the experimental value is 2.55×10^{-2} $\mu\Omega$ cm/°K. The predicted values of the thermoelectric power are small and positive, whereas the measured values are small but negative.[50]

Similar discrepancies between theoretical and experimental values of the transport properties of liquid metals were observed previously in an extensive study by Sundström.[13] Any difference between theory and experiment was there attributed to errors in the published values of the interference functions used in the calculations. Wiser[51] has shown, however, that the resistivity is extremely dependent upon the precise values chosen for $U(K)$. The small errors present in pseudopotential calculations were shown to lead to significant errors (as large as a factor of 2) in the predicted value of the resistivity. Of greater significance, therefore, is the discrepancy of a factor of three in the resistivity coefficient of liquid indium, a quantity which is quite independent of the choice of potential. On the basis of a similar marked discrepancy for the temperature coefficient of liquid sodium, Greenfield[52] concludes that the Born approximation breaks down in liquid metals.

ACKNOWLEDGMENTS

The authors wish to thank Dr. N. C. Halder for the calculation of the thermoelectric power of In and for many stimulating discussions, and the United States Atomic Energy Commission for financial support under Contract AT(30-1)2560.

[47] A. O. E. Animalu and V. Heine, Phil. Mag. **12**, 1249 (1965).

[48] R. Roll and H. Motz, Z. Metallk. **48**, 272 (1957).

[49] E. Scala and W. D. Robertson, Trans. AIME **197**, 1141 (1953).

[50] C. C. Bradley, Phil. Mag. **7**, 1337 (1962).

[51] N. Wiser, Phys. Rev. **143**, 393 (1966).

[52] A. J. Greenfield, Phys. Rev. Letters **16**, 6 (1966).